

## Photochemistry

## Simple and Versatile Molecular Donors for Organic Photovoltaics Prepared by Metal-Free Synthesis

Andreea Diac,<sup>[a, b]</sup> Dora Demeter,<sup>[a]</sup> Magali Allain,<sup>[a]</sup> Ion Grosu,<sup>[b]</sup> and Jean Roncali<sup>\*[a]</sup>

**Abstract:** Donor–acceptor molecules (D- $\pi$ -A) built by connecting a diphenylhydrazone block to a dicyanovinyl acceptor group via various thiophene-based  $\pi$ -conjugating spacers (1–5) were synthesized from mono- or dialdehydes by a simple metal-free procedure. Cyclic voltammetry and UV/Vis absorption spectroscopy show that the extension and/or increase of the donor strength of the spacer produces a decrease of the HOMO and LUMO energy level, a red shift of the absorption spectrum and an increase of the molecular absorption coefficient. Compared to solutions, the optical spectra of spin-cast thin films of compounds 1–3 show a broadening and red shift of the absorption bands, consis-

tent with the formation of J-aggregates. In contrast the blue shift observed for the EDOT-containing compounds 4 and 5 suggests the presence of H-aggregates. Solution-cast and vacuum-deposited films of donors 1–5 were evaluated in solar cells with fullerene C<sub>60</sub> as acceptor. A power-conversion efficiency among the highest reported for bilayer devices of basic configuration was obtained with compound 2. On the other hand, the results obtained with 4 and 5 suggest that the presence of EDOT in the structure can have deleterious effects on the organization and performances of the donor material.

## Introduction

The design and synthesis of active materials for organic photovoltaic cells (OPV) is a focus of considerable current interest motivated by the possibility of producing solar electricity using light-weight, cost-effective and environmentally friendly solar cells.<sup>[1]</sup> The heterojunction generated by contacting an electron donor material (D) with an electron acceptor (A) is the heart of an OPV cell.<sup>[2–5]</sup> In such a system excitons resulting from the absorption of solar photons are dissociated into positive and negative charges by the electrical field at the D–A interface. Over the past two decades this concept has been developed along two main lines namely planar heterojunctions (PHJs)<sup>[4]</sup> initially described by Tang,<sup>[4a]</sup> and bulk heterojunctions (BHJs) in which the D–A interface is distributed in the whole volume of the active layer as interpenetrated networks of D and A materials.<sup>[5]</sup> The fabrication of PHJs and BHJs basically resorts to two different technologies namely thermal evaporation under high vacuum for PHJs and solution-process for BHJs. While these two techniques present specific advantages and drawbacks, they also suggest two different viewpoints on OPV. The relatively expensive fabrication of multilayer cells by successive

vacuum depositions seems to imply the production of durable solar modules, while the production of cheap devices using, for example, ink-jet printing on flexible substrates suggests possible applications in short-lifetime products such as packaging. On the other hand, these two different technologies imply that besides light-absorption and energy levels, the design of active materials takes also into account physical parameters such as melting and decomposition temperature, solubility and film-forming ability.

Although soluble conjugated polymers remain a major class of donor materials for solution-processed BHJs,<sup>[1–3,5]</sup> molecular donors have recently emerged on the forefront of the chemistry of OPV materials due to the advantages of well-defined chemical structures in terms of reproducibility of synthesis, purification and properties combined with possible analyses of structure–properties relationships.<sup>[6]</sup> Furthermore, with adequate structural design, molecular donors present the advantage of being compatible with both processing techniques. In recent years the performances of OPV cells have increased rapidly to reach values of approximately 9.0% for solution-processed single-junction BHJs<sup>[7]</sup> and about 7.0–8.0% for vacuum-deposited PHJs.<sup>[8]</sup> This progress results from a multidisciplinary research efforts involving both device technology (introduction of multiple optimized buffer layers,<sup>[8b]</sup> additives,<sup>[9]</sup> replacement of fullerene C<sub>60</sub> by C<sub>70</sub>-based acceptors<sup>[7–9]</sup>) as well as the development of new donor materials.<sup>[1–3,6–8]</sup> Although these results have clearly established the scientific credibility of OPV, the industrial future of this technology will depend for a large part on the possibility to offer decisive economic and environmental advantages over the well-established silicon solar cells. In this context, the synthesis of active materials by methods com-

[a] A. Diac, Dr. D. Demeter, M. Allain, Dr. J. Roncali  
Group Linear Conjugated Systems, CNRS Moltech-Anjou  
University of Angers  
2 Boulevard Lavoisier 49045 Angers (France)  
E-mail: jeanroncali@gmail.com

[b] A. Diac, Prof. I. Grosu  
Babes Bolyai University, Center of Supramolecular Organic  
and Organometallic Chemistry (CSOOMIC)  
Cluj-Napoca, 11 Arany Janos Street, 400028 Cluj-Napoca (Romania)

binning high yields, scalability, compatibility with industrial processes, low environmental impact and low cost represents a challenging task for chemists interested in OPV.<sup>[10]</sup>

The most efficient polymeric or molecular donor materials known to date are generally obtained by multistep syntheses involving cross-coupling reactions of aromatic organometallic reagents containing magnesium, zinc or tin with metal catalysts such as nickel or palladium.<sup>[10c]</sup> Besides the toxicity and cost of some of these reagents and catalysts, the presence of remnant traces of metal is known to have deleterious effects on the performances of organic semiconductors,<sup>[11]</sup> and thus implies additional purification steps. In this context, the limitation of the overall number of synthetic steps and in particular of those involving metal-catalysed coupling reactions appears as an interesting goal.

It has been shown recently that efficient PHJ cells can be fabricated with push–pull molecules of relatively simple structure such as merocyanines,<sup>[8a]</sup> or triarylamine derivatives.<sup>[8c,d]</sup> In our continuing interest in the design of molecular donors combining structural simplicity, high overall yield and clean synthesis,<sup>[12]</sup> we report here on a series of new D–A molecules in which a diphenylhydrazone donor block is connected to a dicyanovinyl acceptor through  $\pi$ -conjugating spacers based on thiophene (1), bithiophene (2), thieno[3,4*b*]thiophene (3), 3,4-ethylenedioxythiophene (EDOT; 4) and Bis-EDOT (5) (Figure 1). These compounds combine the advantage of a simple, clean and efficient synthesis with physical properties that allow their implementation into devices using both vacuum deposition and solution process. The synthesis and characterization of the electronic properties of the molecules by UV/Vis spectroscopy and cyclic voltammetry are described and the results of a first evaluation of their potential as donor material in PHJ cells are discussed in terms of structure–properties relationships.

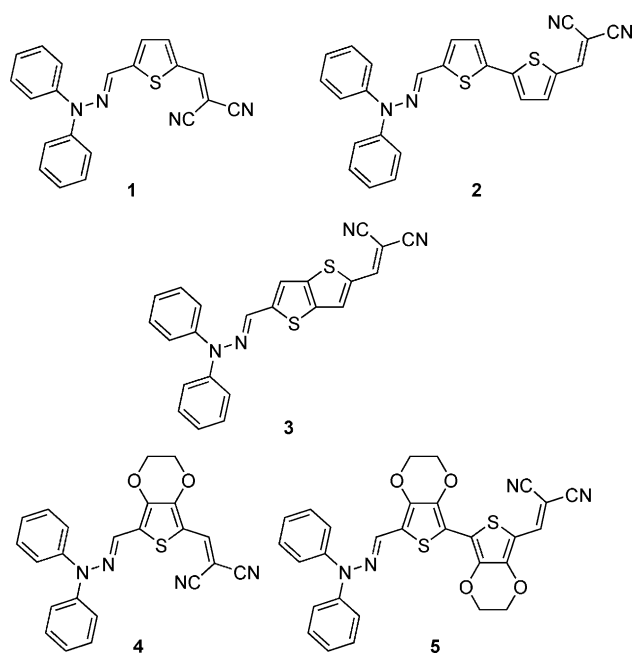


Figure 1. Chemical structure of the target D–A compounds.

## Results and Discussion

The synthesis of the target compounds is depicted in Scheme 1. Treatment of 0.5 equivalent of *N,N*-diphenylhydrazine (9) with one equivalent of 2,5-thiophene dicarboxaldehyde (11a) in THF/methanol at low temperature gave aldehyde 6a in 62% yield (based on 9) together with 21% of the bis-adduct 10a while 18% of the starting dialdehyde 11a was recovered.<sup>[12d]</sup> Application of the same procedure to diformylbithiophene 11b<sup>[13]</sup> gave the bis-adduct 10b and aldehyde 6b in 17 and 37% yield, respectively. Condensation of *N,N*-diphenylhydrazine (9) with monoaldehydes of thienothiophene (8c), EDOT (8d) and bis-EDOT (8e) gave compounds 7c, 7d and 7e in 51 to 63% yields. Finally, a Knoevenagel condensation of aldehydes 6a–e with malonodinitrile gave the target compounds 1–5 in 62 to 96% yields.

### X-ray diffraction

Deep red single crystals for compounds 1, 2 and 3 were grown by slow evaporation from chloroform solutions. The results of single crystal X-ray diffraction analysis are presented in Table 1.

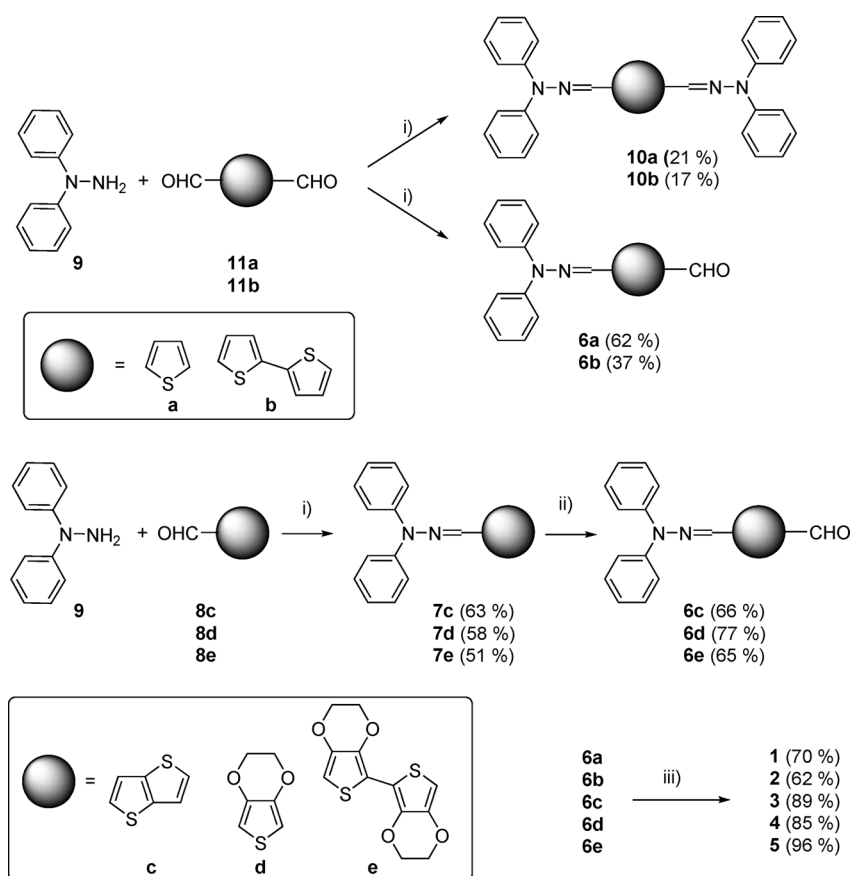
Table 1. Crystallographic data, details of data collection, and structure refinement parameters for compounds 1–3.<sup>[22]</sup>

Compd	1	2	3
formula	C <sub>21</sub> H <sub>14</sub> N <sub>4</sub> S	C <sub>51</sub> H <sub>33</sub> Cl <sub>3</sub> N <sub>6</sub> S <sub>4</sub>	C <sub>23</sub> H <sub>14</sub> N <sub>4</sub> S <sub>2</sub>
<i>M</i> [g mol <sup>-1</sup> ]	354.42	992.44	410.50
<i>T</i> [K]	293 (2)	293 (2)	293 (2)
crystal system	monoclinic	triclinic	monoclinic
space group	<i>P</i> 2 <sub>1</sub> / <i>n</i>	<i>P</i> $\bar{1}$	<i>C</i> <sub>2</sub> / <i>c</i>
<i>a</i> [Å]	11.802 (1)	5.4939 (5)	35.046 (7)
<i>b</i> [Å]	8.7604 (8)	14.717 (1)	8.817 (2)
<i>c</i> [Å]	18.7063 (8)	16.805 (1)	13.733 (2)
$\alpha$ [°]	90	86.677 (7)	90
$\beta$ [°]	106.836 (5)	82.864 (7)	101.81 (1)
$\gamma$ [°]	90	85.485 (7)	90
<i>V</i> [Å <sup>3</sup> ]	1851.2 (2)	1342.44 (17)	4153.7 (14)
<i>Z</i>	4	1	8
$\rho_{\text{calcd}}$ [g cm <sup>-3</sup> ]	1.272	1.228	1.313
$\mu$ [mm <sup>-1</sup> ]	0.186	0.367	0.273
GoF on <i>F</i> <sup>2</sup>	1.111	0.976	1.068
Final <i>R</i> <sub>1</sub> / <i>wR</i> <sub>2</sub> [ <i>I</i> > 2 $\sigma$ ( <i>I</i> )]	0.0443/0.0874	0.0742/0.1940	0.0599/0.0849
<i>R</i> <sub>1</sub> / <i>wR</i> <sub>2</sub> (all data)	0.0779/0.1011	0.1396/0.2208	0.1505/0.1074

As shown in Figure 2, for the three compounds the C=N double bond connecting the hydrazone donor block to the thiophenic spacer presents an *E* configuration.

The three compounds crystallize in centrosymmetric space groups, with one independent molecule in the asymmetric unit, compounds 1 and 3 in the monoclinic system and 2 in the triclinic system. The planarity of the three molecules was evaluated by comparing the dihedral angles between the least-square planes of the three fragments: the donor, the  $\pi$ -conjugated spacer and the acceptor (Figure 3).

In the crystal the molecules of 1 are interconnected into 2D sheets by hydrogen bonding between the hydrogen atom of



**Scheme 1.** Synthesis of the target compounds 1–5. i) AcONa, MeOH/THF; ii) POCl<sub>3</sub>, DMF, 1,2-dichloroethane; iii) CH<sub>2</sub>(CN)<sub>2</sub>, Et<sub>3</sub>N, CHCl<sub>3</sub>.

the dicyanovinyl group and the nitrogen atom of the same group of a neighbouring molecule (N4...H4 2.619(2) Å) and by C–H... $\pi$  interactions between aromatic –CH and neighbouring phenyl ring (C–H19...centroid 3.006(1) Å, C–H14...centroid 3.420(1) Å (Figure 4).

The crystal packing of compound 2 reveals the presence of two types of H bonds between the nitrogen atoms of the CN groups and one hydrogen of the vinyl group (N2...H4 2.723(3) Å) and the other with the iminic hydrogen (N1...H13 2.650(4) Å) (Figure 5).

For compound 3, the crystallographic structure reveals three types of intermolecular interactions namely sulfur–sulfur interactions between thiophene rings (S2...S2 3.376(1) Å), H bonds between one nitrogen atom of the CN groups with one H of the vinyl group (N4...H20 2.68 Å) and the other H atom of the thienothiophene ring (N4...H18 2.688(3) Å) and  $\pi$  stacking (centroid...centroid 3.788(1) Å, centroid S2/C16–C19; Figure 5). In the crystal lattice supramolecular dimers with head-to-tail arrangement sustained by  $\pi$  stacking are observed. These dimers are further interconnected by H bonds and S...S interactions into supramolecular chains (Figure 6).

### UV/Vis absorption spectroscopy

Figure 7 shows the UV/Vis absorption spectra of compounds 1–5 in methylene chloride solution and as thin films spin-cast

on glass. The spectrum of all compounds presents a first absorption band around 350–400 nm followed by a more intense band in the 500–600 nm region attributed to an internal charge transfer (ICT).

As shown by the data in Table 2, the increase of the conjugation length and/or donor strength of the conjugating spacer produces a bathochromic shift of the absorption maximum ( $\lambda_{\text{max}}$ ) of the ICT band from 507 to 574 nm for 1 and 5, respectively, with an increase of the molecular absorption coefficient ( $\epsilon$ ). Comparison of these spectra to those of the corresponding spin-cast films reveals two different behaviours. For compounds 1–3, the solid-state spectrum presents a broadening of the absorption bands with a bathochromic shift of  $\lambda_{\text{max}}$ . These phenomena commonly observed for many classes of molecular or polymeric conjugated systems are generally attributed to intermolecular interactions with formation of J-aggregates. In contrast

the solid-state spectra of the EDOT-containing compounds 4 and 5 show narrower absorption bands with a hypsochromic shift of  $\lambda_{\text{max}}$  in particular for compound 5 (14 nm; Table 2). This peculiar behaviour which suggests the presence of H-aggregates has been previously observed for other EDOT-containing systems such as hybrid EDOT–thiophene oligomers<sup>[14]</sup> or push–pull molecules.<sup>[15]</sup> Although these results provide a further illustration of the major contribution of EDOT units on the formation of H-aggregates, a general explanation of this process is still lacking and would require further analyses of structure–properties relationships.

### Cyclic voltammetry

Figure 8 shows the oxidative cyclic voltammograms (CV) of compounds 1–5 in CH<sub>2</sub>Cl<sub>2</sub> in the presence of tetrabutylammonium hexafluorophosphate as supporting electrolyte. The CV of all compounds presents a first oxidation peak corresponding to the formation of the cation radical.

As expected, the extension of the spacer or the increase of its donor strength by insertion of EDOT units produces a large negative shift of the anodic peak potential ( $E_{\text{pa}}$ ) from 1.32 V for compound 1 to 0.79 V for compound 5 (Table 2). In this latter case the CV shows two reversible oxidation waves indicative of stable cation-radical and dication. A closer examination of the CVs shows that except for compound 5, the oxidation process

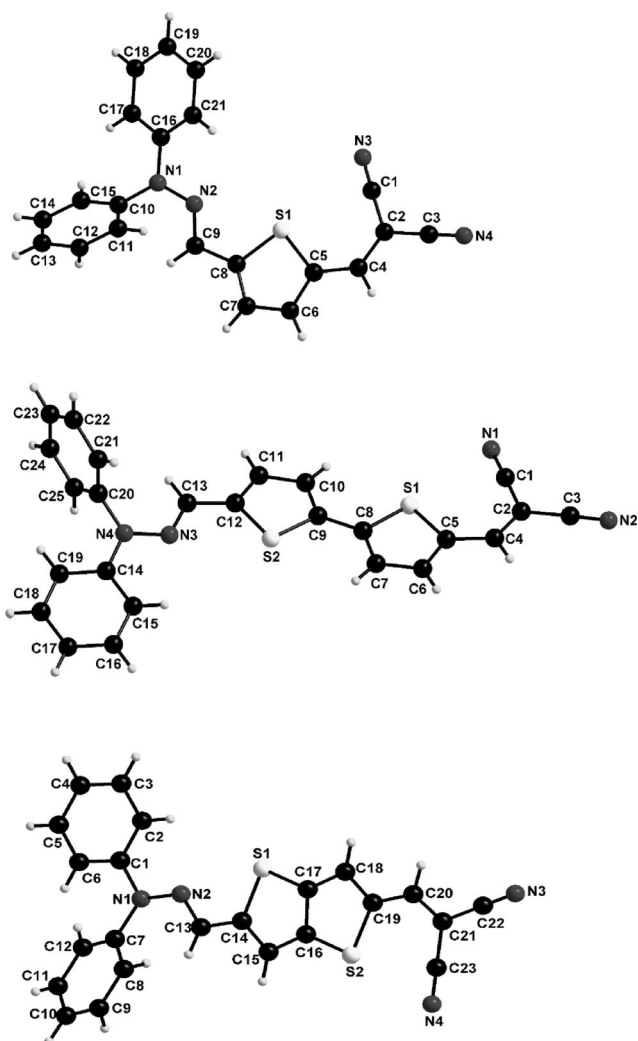


Figure 2. Crystallographic structure of compounds 1 (top), 2 (middle) and 3 (bottom).

is not fully reversible and that a cathodic wave of weak intensity is observed in the reverse scan. This wave, particularly visible in the CV of compound 1 and hardly discernible in the case of compound 2 can be attributed to the reduction of the product resulting from the coupling of the cation radical, a process frequently observed in the electrochemistry of TPA derivatives.<sup>[17]</sup> In the negative potential region, the CV of all compounds (data not shown) present an irreversible reduction wave with a cathodic peak potential ( $E_{pc}$ ) varying from  $-0.91$  V for compound 1 to  $-1.17$  V for compound 5 (Table 2). The

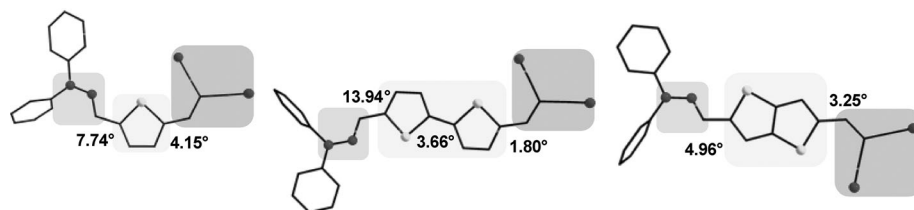


Figure 3. Dihedral angles between the three constitutive blocks of the conjugated system of compounds 1–3.

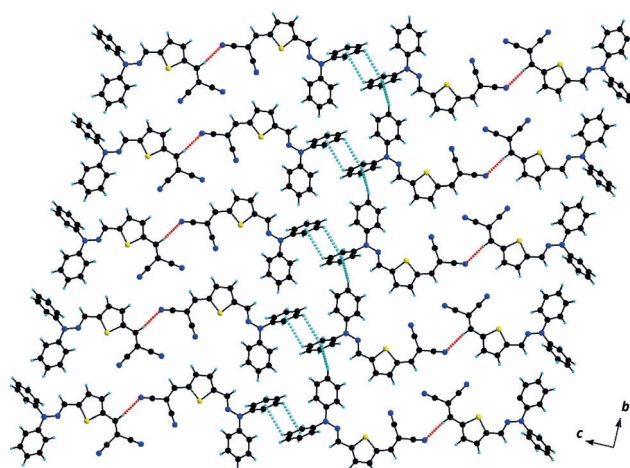


Figure 4. Crystal packing in 1: 2D layer generated by hydrogen bonds (red dashed line) and C–H... $\pi$  interactions (cyan dashed line).

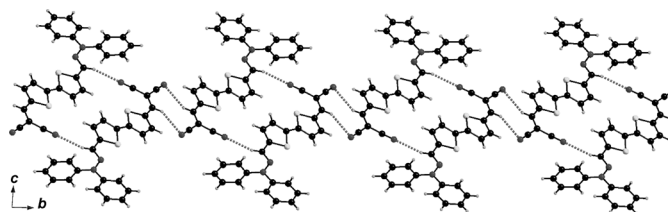


Figure 5. Supramolecular chain generated by hydrogen bonds in the crystal of compound 2.

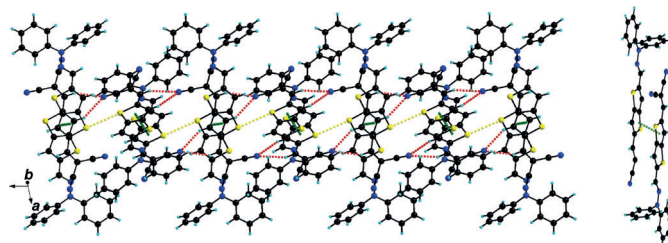
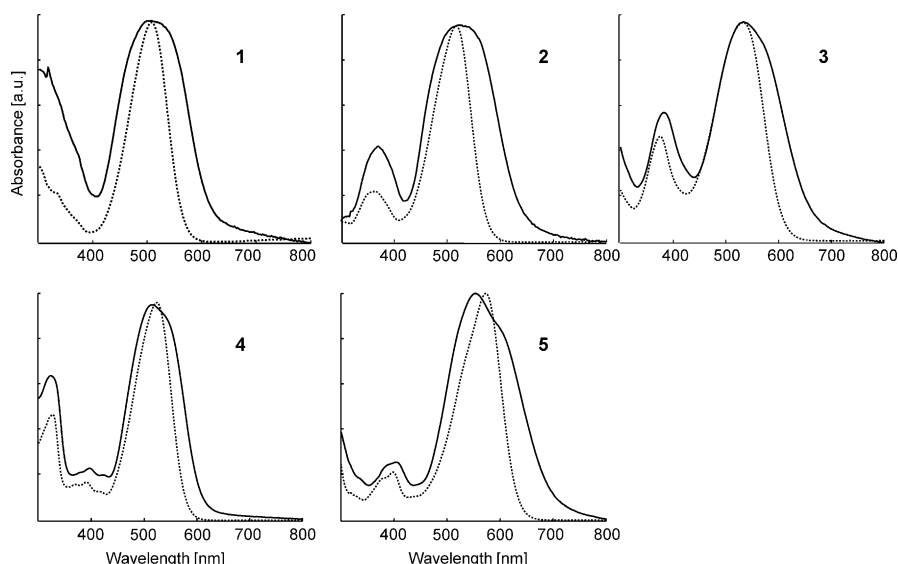


Figure 6. Crystal packing of compound 3 showing S...S interactions (yellow dashed line), hydrogen bonding (red dashed line) and  $\pi$  stacking (green dashed line).

energy levels of the frontier orbitals were estimated from the oxidation potentials and the optical data. For all compounds the level of the LUMO is compatible with a photoinduced electron transfer into the LUMO of  $C_{60}$ .

### Evaluation of photovoltaic performances

Compounds 1–5 were evaluated as donor materials in bilayer PHJs of  $0.28$  cm<sup>2</sup> active area with vacuum-deposited  $C_{60}$  as electron acceptor. Although solution-processed BHJs are known



**Figure 7.** Normalized UV/Vis absorption spectra of compounds 1–5. Dotted lines: in  $\text{CH}_2\text{Cl}_2$ . Solid lines: thin films spin-cast on glass from chloroform solutions.

**Table 2.** Data of UV/Vis spectroscopy (s):  $\sim 1 \times 10^{-5}$  M in  $\text{CH}_2\text{Cl}_2$ ; (f): films spin-cast on glass, and cyclic voltammetry (in 0.10 M  $\text{Bu}_4\text{NPF}_6/\text{CH}_2\text{Cl}_2$ , scan rate  $100 \text{ mV s}^{-1}$ , Pt electrodes, reference SCE).

Donor	$\lambda_{\text{max}}$ (s) [nm]	$\Delta E$ [eV]	$\epsilon_{\text{max}}$ [ $\text{M}^{-1} \text{cm}^{-1}$ ]	$\lambda_{\text{max}}$ (f) [nm]	$E_{\text{g}}$ [eV]	$E_{\text{pa}}$ [V]	$E_{\text{pc}}$ [V]	$E_{\text{HOMO}}$ [eV] <sup>[b]</sup>	$E_{\text{LUMO}}$ [eV] <sup>[c]</sup>
1 <sup>[a]</sup>	507	2.44	39 000	520	2.00	1.32	−0.91	−6.01	−3.57
2	533	2.32	32 000	542	1.86	1.02	−1.02	−5.71	−3.39
3	518	2.39	29 000	532	1.92	1.15	−1.02	−5.84	−3.45
4	525	2.35	36 000	520	2.01	1.11	−1.11	−5.80	−3.45
5	574	2.15	47 000	560	1.75	0.79	−1.17	−5.48	−3.33

[a] From ref. [12d]. [b] Using  $E^{\text{ox}}$  with an offset of  $-4.99$  eV for SCE versus the vacuum level.<sup>[16]</sup> [c] Determined by  $E_{\text{HOMO}} - \Delta E$ .

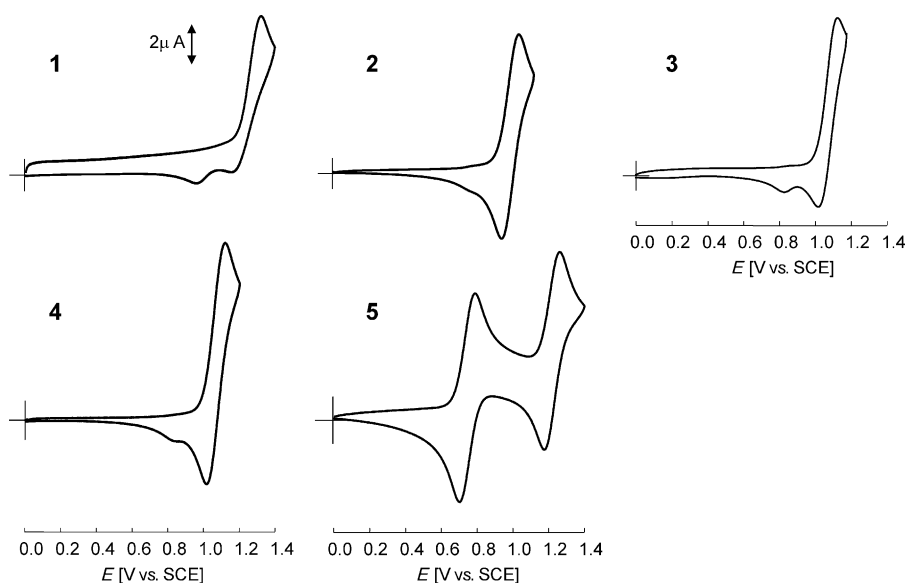


**Figure 8.** Cyclic voltammograms corresponding to the oxidation of compounds 1–5 in 0.10 M  $\text{Bu}_4\text{NPF}_6/\text{CH}_2\text{Cl}_2$ , Pt electrodes, scan rate  $100 \text{ mV s}^{-1}$ .

to reach much higher efficiencies, especially when using small active areas, optimized interfacial layers, additives and  $\text{C}_{70}$  derivatives, such cells require lengthy optimization and hence larger quantities of donor material and they show in general a larger dispersion of results than PHJ cells. In this context, basic PHJs cells appear more appropriate for an analysis of structure–properties relationships. In other words, the purpose of this work is not to produce champion devices but rather to analyse the effects of subtle structural modifications.

The bilayer cells were fabricated by deposition of a donor layer on ITO substrates pre-coated with a 40 nm thick film of spin-cast PEDOT:PSS. The substrates were then introduced in a vacuum chamber, a 30 nm thick layer of  $\text{C}_{60}$  was deposited by thermal evaporation and the devices were completed by deposition of a 100 nm layer of aluminium. Each ITO substrate contains two circular cells and each batch typically involves 6–8 cells. After fabrication the cells were subjected to a 10 min thermal treatment at a temperature of 110 to 160 °C.

An interesting specificity of the new donors lies in the fact that their solubility and melting and decomposition temperatures are compatible with both solution-process and vacuum deposition. It was therefore interesting to take advantage of this processing versatility to compare the performances of OPV cells fabricated by the two techniques. Figure 9 shows the current density versus voltage curves for the cells based on compounds 1–3 and the corresponding photovoltaic parameters are listed in Table 3.

As already reported in a short communication, a cell based on a spin-cast film of 1 (entry 1s) gave a short-circuit current–den-

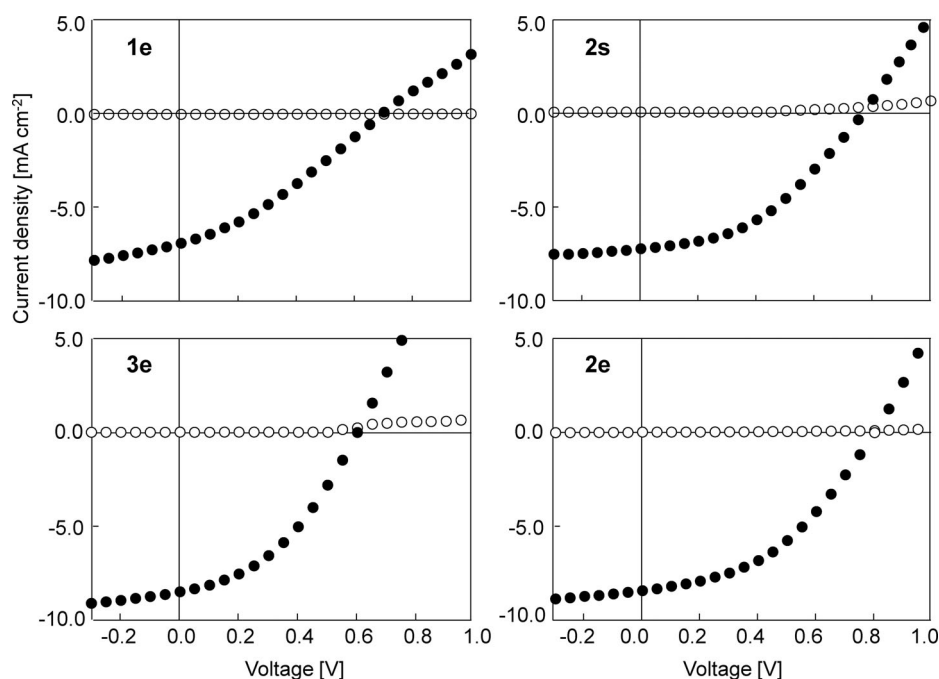


**Figure 9.** Current density versus voltage curves for bilayer photovoltaic cells ITO/PEDOT:PSS/D/C<sub>60</sub>/Al based on spin-cast (s) and 15 nm vacuum-deposited (e) layers of donors 1, 2 and 3. Empty circles: in the dark; filled circles: under AM 1.5 simulated solar illumination with an incident power light of 90 mW cm<sup>-2</sup>.

sity ( $J_{sc}$ ) of 6.32 mA cm<sup>-2</sup> and a power conversion efficiency ( $PCE$ ) of 2.07%.<sup>[12d]</sup> As shown in Table 3, the cells based on vacuum deposited donor 1 (entry 1e) show a slight improvement of  $J_{sc}$  from approximately 6.30 to 6.90 mA cm<sup>-2</sup> but a decrease of  $V_{oc}$  and  $FF$  with as net result a decrease of  $PCE$  to about 1.70%. The results obtained with vacuum-deposited donor 3 reveal a higher of  $J_{sc}$  of 8.50 mA cm<sup>-2</sup>, however the maximum  $PCE$  is limited to 2.30% due to the decrease of  $V_{oc}$  to 0.60 V, in agreement with the higher HOMO level of compound 3. In spite of a correct solubility, the film-forming properties of compound 3 were insufficient to produce a good quality spin-cast film.

Comparison of the data for donors 1 and 2 shows that the insertion of a bithienyl bridge produces an increase of  $PCE$  to 2.55% for the spin-cast film and 3.22% for the vacuum deposited one. This result is due essentially to a better  $FF$  and to an increase of  $J_{sc}$  above 8.0 mA cm<sup>-2</sup>. The relatively high value of  $V_{oc}$  in spite of the higher HOMO level of compound 2 could be due to a higher interfacial dipole or to a decrease of charge recombination. Further work is needed to clarify this point. Comparison of entries 2s and 2e in Table 3 shows that the cells made by vacuum deposition present higher  $J_{sc}$  and  $V_{oc}$  and hence higher  $PCE$ . It is worth noting that the 3.22%  $PCE$  is the highest value obtained so far with our standard 0.28 cm<sup>2</sup> bilayer device. Taking into account the large increase of  $PCE$  achieved by optimization of cells based on other small TPA-based donors,<sup>[18]</sup> these first results suggest that there is still much room for improvement.

The results obtained with the cells based on donors 4 and 5 show that the replacement of the thiophenes by EDOT units has deleterious consequences for the PV performances

(Figure 10). Comparison of the data for compounds 1 and 4 reveals a decrease of  $PCE$  for both solution-cast and vacuum-deposited donor layers due essentially to a decrease of  $V_{oc}$  associated with the higher HOMO level of compound 4. On the other hand, the results obtained with donors 2 and 5 show that the replacement of bithienyl spacer by a bis-EDOT produces an even larger decrease of  $J_{sc}$  with a two-fold decrease of  $PCE$  for solution-processed devices while  $J_{sc}$  decreases from 8.40 to 2.17 mA cm<sup>-2</sup> and  $PCE$  from 3.22 to 0.65% for the cells based on the vacuum-deposited donors layers.

Comparison of the results obtained with solution-cast and vacuum-deposited donor layers reveals two contrasted situations. For compounds 1 and 2, vacuum deposition improves  $J_{sc}$  while the reverse effect is observed for the EDOT-containing donors in particular for compound 5 for which vacuum-deposition leads to a considerable deterioration of the PV performances.

In order to complete these observations, the external quantum efficiency ( $EQE$ ) spectra of the cells were recorded under monochromatic irradiation. The spectra of all devices show

**Table 3.** Photovoltaic characteristics of PHJ bilayer cells ITO/PEDOT:PSS/D/C<sub>60</sub>/Al under AM 1.5 simulated solar irradiation with an incident power light of 90 mW cm<sup>-2</sup>.<sup>[a]</sup>

Compd	An. temp. [°C]	$J_{sc}$ [mA cm <sup>-2</sup> ]	$V_{oc}$ [V]	$FF$ [%]	$PCE$ [%]
1s <sup>[a]</sup>	110	6.40	0.75	33	1.76
1s <sup>[a]</sup>	110	<b>6.32</b>	<b>0.79</b>	<b>37</b>	<b>2.07</b>
1e	110	6.83	0.68	32	1.64
1e	110	<b>6.87</b>	<b>0.69</b>	<b>32</b>	<b>1.68</b>
2s	120	7.32	0.74	40	2.41
2s	120	<b>7.14</b>	<b>0.76</b>	<b>42</b>	<b>2.55</b>
2e	120	8.73	0.77	40	3.06
2e	120	<b>8.42</b>	<b>0.80</b>	<b>43</b>	<b>3.22</b>
3e	140	7.71	0.61	41	2.15
3e	140	<b>8.53</b>	<b>0.60</b>	<b>40</b>	<b>2.28</b>
4s	150	5.68	0.66	29	1.28
4s	150	<b>6.19</b>	<b>0.63</b>	<b>35</b>	<b>1.47</b>
4e	160	4.78	0.69	29	1.05
4e	160	<b>5.25</b>	<b>0.69</b>	<b>30</b>	<b>1.20</b>
5s	160	5.65	0.63	32	1.22
5s	160	<b>5.30</b>	<b>0.54</b>	<b>41</b>	<b>1.30</b>
5e	160	2.12	0.66	39	0.63
5e	160	<b>2.17</b>	<b>0.70</b>	<b>39</b>	<b>0.65</b>

[a] Data in italics are the average of 6–8 cells, data in bold are the best results for each series. An. temp = annealing temperature.

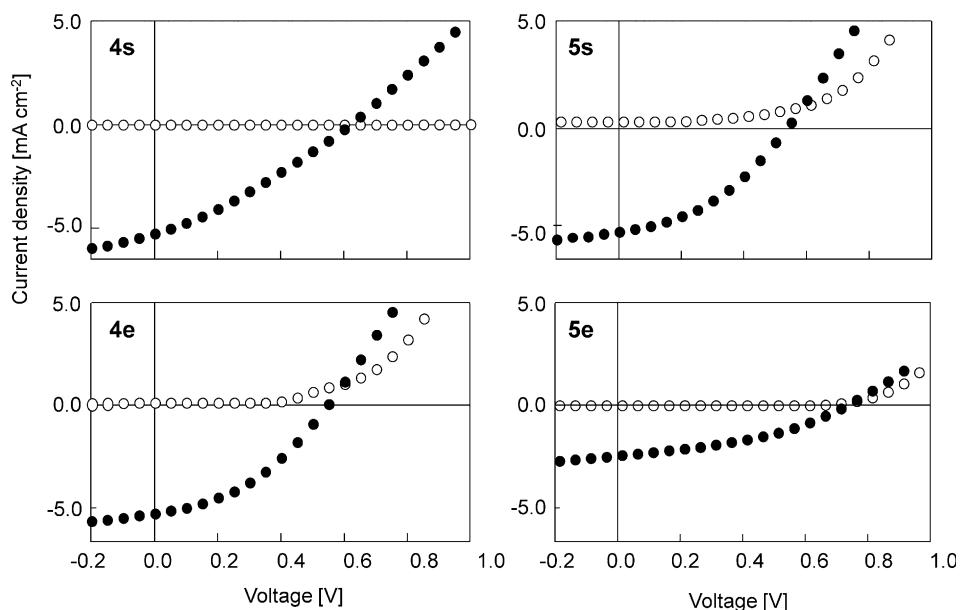


**Figure 10.** Current density versus voltage curves for bilayer solar cells (ITO/PEDOT:PSS/D/C<sub>60</sub>/aluminium. In the dark (open circles) and under simulated solar light with incident power light of 90 mW cm<sup>-2</sup> (black circles).

a first sharp peak at 370–380 nm attributed to the contribution of C<sub>60</sub> to the photocurrent. The spectrum of the cell based on vacuum-deposited compound **1** shows a first band at 400 nm followed by a broader band of about 50% extending to about 600 nm (Figure 11). The response of compound **3e** is rather similar to that of **1e** and both are consistent with the absorption spectra of the donors.

The spectrum of the cells based on donor **2** shows, as expected, an extension of the photoresponse with a bathochro-

wavelengths. However, a marked decrease of *EQE* is observed in the 500–700 nm region for the vacuum-deposited donor. These *EQE* spectra agree well with the results obtained under white-light illumination and clearly confirm the negative influence of the bis-EDOT spacer on the conversion efficiency of the donor molecule.

Previous work on hybrid thiophene–EDOT oligomers has shown that the number and position of EDOT units in the conjugated structure exerts a determining influence on the molec-

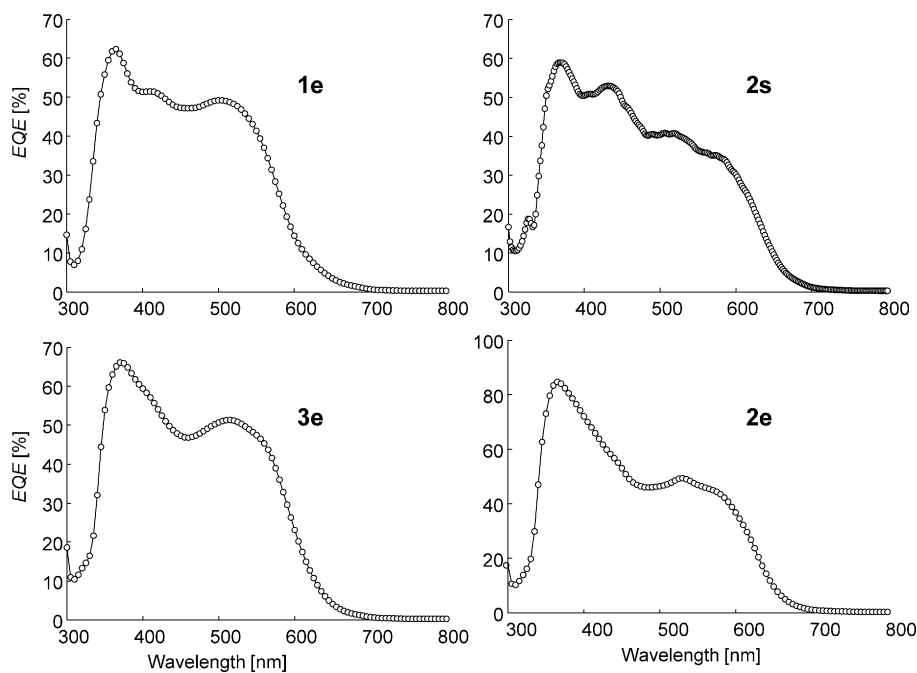


**Figure 11.** Spectra of external quantum efficiency of bilayer cells based on donors **1**, **2** and **3** under monochromatic irradiation.

mic shift of the onset of photocurrent to approximately 650 nm. The *EQE* spectra of the cells based on solution-cast and vacuum-deposited donor layers are rather similar except for a slightly higher intensity for the vacuum-deposited donor (Figure 11).

As shown in Figure 12, the processing technique has a much stronger effect in the case of EDOT-containing donors. For compound **4** the *EQE* spectra of both types of cells have almost identical shape with a lower photocurrent for the vacuum-deposited donor. For compound **5**, the spectra of the solution-processed and vacuum-deposited donors present as expected, an extension of the photoresponse towards longer

wavelengths. However, a marked decrease of *EQE* is observed in the 500–700 nm region for the vacuum-deposited donor. These *EQE* spectra agree well with the results obtained under white-light illumination and clearly confirm the negative influence of the bis-EDOT spacer on the conversion efficiency of the donor molecule.

Previous work on hybrid thiophene–EDOT oligomers has shown that the number and position of EDOT units in the conjugated structure exerts a determining influence on the molecular organization and in particular on the formation of J- or H-aggregates.<sup>[14,15]</sup> In fact, results on OFETs and OPV cells have shown that the spectral signature of H-aggregates is associated with a higher hole-mobility in OFETs but with a dramatic loss of the light-harvesting properties and hence *PCE* of OPV cells.<sup>[14]</sup> In this context the results obtained with compounds **4** and **5** provide a further illustration of the problems posed by use of the EDOT building block for the design of OPV materials, even if interesting positive effects have been demonstrated in some cases.<sup>[15]</sup>

Although our results confirm the versatile processibility of this class of molecular donors, they also show that depending on the molecular structure, the processing technique can exert

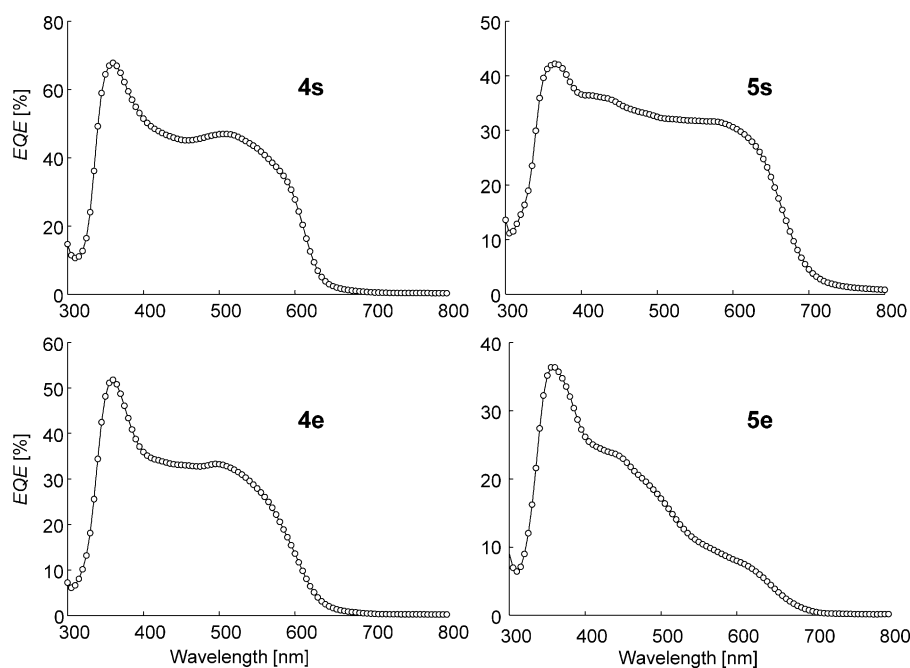


**Figure 12.** Spectra of external quantum efficiency of bilayer cells based on donors **4**, and **5** under monochromatic irradiation. Spun-cast (s) donor layer and vacuum-deposited (e) donor layer are shown.

a significant influence on the efficiency of the resulting OPV cell. Thus, whereas for compound **1** both methods lead to rather similar results, for compound **2** vacuum deposition leads to a about 25% higher *PCE* due essentially to an increase of  $J_{sc}$ . In contrast, for compounds **4** and **5** vacuum-deposition seems to exalt the deleterious influence of the EDOT unit on molecular packing and hence PV performances.

## Conclusion

To summarize, new push-pull molecules have been synthesized in good yields by a simple and straightforward metal-free procedure. Electrochemical and optical results show that the nature and length of the conjugating spacer exert a determining influence on the energy levels and light-harvesting properties of the molecule. A first evaluation of the potential of the compounds as donor material in simple bilayer cells has confirmed the determining role of the conjugating bridge on conversion efficiency. The results obtained with EDOT-containing molecules have confirmed the difficulty to predict the effects of this building block on the organization of the material and hence on its electronic properties and photovoltaic performances. On the other hand, the results obtained with donors based on thiophenic spacers and in particular bithiophene suggest that these materials can represent an interesting trade-off when considering the balance of conversion efficiency and the cost, simplicity, cleanness, yield and scalability of the synthesis and the processing versatility. Work devoted to the optimization of the synthetic steps, to the extension of this synthetic approach, to molecules with improved photovoltaic parameters and to the fabrication of optimized PHJ and BHJ

cells using the most promising compounds of this study is now underway and will be reported elsewhere.

## Experimental Section

### General

NMR spectra were recorded with a Bruker AVANCE III 300 ( $^1\text{H}$ , 300 MHz and  $^{13}\text{C}$ , 75 MHz). Chemical shifts are given in ppm relative to TMS. UV/Vis spectra were recorded with a Perkin-Elmer Lambda 19 or 950 spectrometer. Melting points are uncorrected. Matrix-assisted laser desorption/ionization was performed on MALDI-TOF MS BIFLEX III Bruker Daltonics spectrometer using di-thranol as matrix.

Cyclic voltammetry was performed in dichloromethane solution purchased from SDS (HPLC grade). Tetrabutylammonium hexafluorophosphate (0.10 M as supporting electrolyte) was purchased from Acros and was used without purification. Solutions were deaerated by nitrogen bubbling prior to each experiment. Experiments were carried out in a one-compartment cell equipped with platinum electrodes and saturated calomel reference electrode (SCE) with a Biologic SP-150 potentiostat with positive feedback compensation.

### Synthesis

Compounds **1**,<sup>[12d]</sup> **11 a**,<sup>[13]</sup> **11 b**,<sup>[13]</sup> **8 c**,<sup>[19]</sup> **8 d**<sup>[20]</sup> and **8 e**<sup>[21]</sup> were obtained using known procedures. While all final compounds are obtained by Knoevenagel condensation of malonodinitrile with the appropriate aldehyde, these aldehydes were obtained along two main routes. In the case of compounds **1** and **2** treatment of diphenylhydrazine **9** with dialdehydes **11 a** and **11 b** gives a mixture of the double condensation product **10 a** and **10 b** and of the expected aldehyde **6 a** or **6 b**. The use of a twofold excess of dialdehyde and of diluted reaction medium allows the orientation of the reaction towards the desired aldehyde and limitation of the formation of by-products **10 a** and **10 b** while a large part of the starting dialdehyde can be recovered.

#### *5,5'-Bis((E)-(2,2-diphenylhydrazono)methyl)-2,2'-bithiophene (10 b)*

To a solution of [2,2'-bithiophene]-5,5'-dicarbaldehyde (**11 b**; 470 mg, 2.11 mmol) in 120 mL dry THF warmed to 25 °C was added a solution of *N,N'*-diphenylhydrazine hydrochloride (**9**; 233 mg, 1.05 mmol) and sodium acetate (346 mg, 4.22 mmol) in 30 mL anhydrous methanol. The reaction mixture was stirred for three days at 25 °C under argon atmosphere. After being cooled to room temperature, the mixture was diluted with methylene chloride and washed with water and brine. After removal of solvent the residue was chromatographed on silica gel using methylene chloride as eluent to give 100 mg (17%) of a yellow powder. M.p: 268–269 °C;  $^1\text{H}$  NMR (300 MHz,  $\text{CDCl}_3$ ):  $\delta$  = 7.46–7.41 (m, 8H), 7.24–

7.18 (m, 14H), 7.08 (d, 2H,  $J=3.6$  Hz), 6.80 ppm (d, 2H,  $J=3.9$  Hz);  $^{13}\text{C}$  NMR (75 MHz,  $\text{CDCl}_3$ ):  $\delta=143.4, 141.0, 137.3, 130.2, 130.0, 127.3, 124.9, 124.0, 122.6$  ppm; MS (MALDI-TOF): 554.4  $[M]^+$ ; HRMS (FAB): elemental analysis calcd (%): 554.1599; found: 554.1601.

**(E)-5'-((2,2-Diphenylhydrazono)methyl)-[2,2'-bithiophene]-5-carbaldehyde (6b)**

The same reaction gave after chromatography 150 mg (37%) of an orange powder. M.p.: 140–141 °C;  $^1\text{H}$  NMR (300 MHz,  $\text{CDCl}_3$ ):  $\delta=9.85$  (s, 1H), 7.67 (d, 1H,  $J=3.9$  Hz), 7.47–7.42 (m, 4H), 7.28 (d, 1H,  $J=3.9$  Hz), 7.25–7.18 (m, 8H), 6.83 ppm (d, 1H,  $J=3.9$  Hz);  $^{13}\text{C}$  NMR (75 MHz,  $\text{CDCl}_3$ ):  $\delta=182.6, 147.5, 144.0, 143.1, 141.7, 137.6, 135.2, 130.1, 129.3, 127.1, 126.5, 125.2, 124.3, 122.6$  ppm; MS (MALDI-TOF): 388.2  $[M]^+$ ; HRMS (MALDI-TOF): elemental analysis calcd (%): 388.0704; found: 388.0702.

**(E)-2-((5'-((2,2-Diphenylhydrazono)methyl)-[2,2'-bithiophen]-5-yl)methylene)malononitrile (2)**

Malonodinitrile (69 mg, 1.04 mmol) and few drops of triethylamine were added to a solution of aldehyde **6b** (200 mg, 0.52 mmol) in 70 mL chloroform and the mixture was heated at 62 °C for 15 h. After cooling to room temperature, the reaction mixture was diluted with methylene chloride, washed with water and brine and dried over anhydrous  $\text{MgSO}_4$ . After solvent removal, the residue was purified by column chromatography (silica gel, eluent: dichloromethane/petroleum ether=4:1) to give 140 mg (62%) of a deep violet powder. M.p.: 206–208 °C;  $^1\text{H}$  NMR (300 MHz,  $\text{CDCl}_3$ ):  $\delta=7.75$  (s, 1H), 7.64 (d, 1H,  $J=4.2$  Hz), 7.50–7.45 (m, 4H), 7.32 (d, 1H,  $J=4.2$  Hz), 7.30 (d, 1H,  $J=3.9$  Hz), 7.28–7.27 (m, 1H), 7.25–7.20 ppm (m, 7H);  $^{13}\text{C}$  NMR (75 MHz,  $\text{CDCl}_3$ ):  $\delta=150.1, 149.8, 145.5, 143.0, 140.5, 134.2, 133.5, 130.1, 128.9, 127.8, 127.3, 125.3, 124.6, 122.5, 114.5, 113.7, 75.7$  ppm; MS (MALDI-TOF): 436.1  $[M]^+$ ; HRMS (MALDI-TOF): elemental analysis calcd (%): 436.0816; found: 436.0804.

**(E)-1,1-Diphenyl-2-(thieno[3,2-b]thiophen-2-ylmethylene)hydrazine (7c)**

A solution of *N,N'*-diphenylhydrazine hydrochloride (**9**; 262 mg, 1.19 mmol) and sodium acetate (195 mg, 2.38 mmol) in 8 mL dry methanol was added dropwise to a solution of thieno[3,2-b]thiophene-2-carbaldehyde (**8c**; 200 mg, 1.19 mmol) in 20 mL anhydrous THF. The reaction mixture is stirred, overnight, at room temperature, under argon atmosphere and then it was heated to 70 °C for 4 h. After being cooled to room temperature, the solution was diluted with methylene chloride, washed with water and brine and dried over  $\text{MgSO}_4$ . After solvent removal, the residue was chromatographed on silica gel, using as eluent a mixture of dichloromethane/petroleum ether=2:1 to give 250 mg (63%) of a yellow solid. M.p.: 170–171 °C;  $^1\text{H}$  NMR (300 MHz,  $\text{CDCl}_3$ ):  $\delta=7.46$ –7.41 (m, 4H), 7.35 (d, 1H,  $J=5.1$  Hz), 7.30 (s, 1H), 7.23–7.19 (m, 7H), 7.04 ppm (s, 1H);  $^{13}\text{C}$  NMR (75 MHz,  $\text{CDCl}_3$ ):  $\delta=144.4, 143.4, 139.2, 139.0, 130.6, 130.0, 127.6, 124.9, 122.6, 120.0, 118.6$  ppm; MS (MALDI-TOF): 334.2  $[M]^+$ ; HRMS (MALDI-TOF): elemental analysis calcd (%): 334.0598; found: 334.0588.

**(E)-5-((2,2-Diphenylhydrazono)methyl)thieno[3,2-b]thiophene-2-carbaldehyde (6c)**

Anhydrous DMF (0.08 mL, 1.08 mmol) and phosphorus oxychloride (0.08 mL, 0.9 mmol) were added to a solution of (E)-1,1-diphenyl-2-(thieno[3,2-b]thiophen-2-ylmethylene)hydrazine (**7c**; 200 mg,

0.6 mmol) in 10 mL 1,2-dichloroethane. The reaction mixture was heated to 87 °C for 6 h. After being cooled to room temperature, a saturated aqueous solution of sodium acetate and dichloromethane were added and the mixture was additionally stirred for 2 h. After extraction with  $\text{CH}_2\text{Cl}_2$  (3×50 mL), the combined organic phases were washed with water and brine, dried over  $\text{MgSO}_4$  and concentrated. The residue was purified by column chromatography on silica gel (eluent:  $\text{CH}_2\text{Cl}_2/\text{EP}=2:1$ ) to afford 140 mg (66%) of an orange solid. M.p.: 145–147 °C;  $^1\text{H}$  NMR (300 MHz,  $\text{CDCl}_3$ ):  $\delta=9.92$  (s, 1H), 7.86 (s, 1H), 7.48–7.43 (m, 4H), 7.28 (s, 1H), 7.25–7.19 (m, 6H), 7.06 ppm (s, 1H);  $^{13}\text{C}$  NMR (75 MHz,  $\text{CDCl}_3$ ):  $\delta=183.2, 151.0, 146.3, 145.0, 142.9, 138.5, 130.1, 129.4, 129.1, 125.5, 122.6, 118.4$  ppm; MS (MALDI-TOF): 362.2  $[M]^+$ ; HRMS (MALDI-TOF): elemental analysis calcd (%): 362.0548; found: 362.0550.

**(E)-2-((5'-((2,2-Diphenylhydrazono)methyl)thieno[3,2-b]thiophen-2-yl)methylene)malononitrile (3)**

To a solution of (E)-5-((2,2-diphenylhydrazono)methyl)thieno[3,2-b]thiophene-2-carbaldehyde (**6c**; 120 mg, 0.33 mmol) in 30 mL  $\text{CHCl}_3$ , malonodinitrile (50 mg, 0.75 mmol) and few drops of triethylamine were added. The mixture was stirred under argon atmosphere, at room temperature for 4 h. After removal of solvent, the residue was solubilized in dichloromethane, washed with water and brine, and dried over magnesium sulfate. The resulting solid was washed with cold ethanol, giving 120 mg (89%) of a deep-violet powder. M.p.: 262–264 °C;  $^1\text{H}$  NMR (300 MHz,  $\text{CDCl}_3$ ):  $\delta=7.81$  (d, 2H,  $J=8.4$  Hz), 7.49–7.44 (m, 4H), 7.30–7.19 (m, 7H), 7.05 ppm (s, 1H);  $^{13}\text{C}$  NMR (75 MHz,  $\text{CDCl}_3$ ):  $\delta=153.4, 150.8, 148.7, 142.6, 139.3, 136.7, 130.6, 130.2, 128.6, 125.8, 122.6, 117.8, 114.6, 113.8, 75.5$  ppm; MS (MALDI-TOF): 410.2  $[M]^+$ ; HRMS (MALDI-TOF): elemental analysis calcd (%): 410.0660; found: 410.0650.

**(E)-2-((2,3-Dihydrothieno[3,4-b][1,4]dioxin-5-yl)methylene)-1,1-diphenylhydrazine (7d)**

A mixture of *N,N'*-diphenylhydrazine hydrochloride (1.43 g, 6.46 mmol) and sodium acetate (1.06 g, 12.9 mmol) in 25 mL MeOH was added dropwise to a solution of aldehyde **8d** (1.1 g, 6.46 mmol) in 50 mL dry THF, under argon atmosphere. The reaction mixture was stirred, overnight, at room temperature under inert atmosphere. The mixture was quenched with water and extracted with dichloromethane. The combined organic extracts were washed with water, brine and dried over  $\text{MgSO}_4$ . After solvent removal, the crude was purified by column chromatography on silica gel using a mixture of petroleum ether/dichloromethane=2:1 as eluent to give 1.26 g (58%) of a yellow solid. M.p.: 146–147 °C;  $^1\text{H}$  NMR (300 MHz,  $\text{CDCl}_3$ ):  $\delta=7.43$ –7.37 (m, 4H), 7.27 (s, 1H), 7.19–7.14 (m, 6H), 6.24 (s, 1H), 4.14 ppm ( $s_{\text{br}}$ , 4H);  $^{13}\text{C}$  NMR (75 MHz,  $\text{CDCl}_3$ ):  $\delta=143.6, 141.7, 140.0, 129.9, 127.7, 124.6, 122.5, 116.1, 99.4, 64.9, 64.8$  ppm; HRMS (MALDI-TOF): elemental analysis calcd (%): 336.0932; found: 336.0925.

**(E)-7-((2,2-Diphenylhydrazono)methyl)-2,3-dihydrothieno[3,4-b][1,4]dioxine-5-carbaldehyde (6d)**

To a solution of hydrazone derivative **7d** (0.6 g, 1.78 mmol) in 50 mL 1,2-dichloroethane cooled to 0 °C anhydrous DMF (0.2 mL, 2.5 mmol) and phosphoryl chloride (0.2 mL, 2.14 mmol) were added. The reaction mixture was stirred, overnight, at room temperature. Aqueous solution of sodium acetate and dichloromethane are added and the solution was additionally stirred for 1 h. The organic layer was washed twice with water and dried over  $\text{MgSO}_4$ . After removal of solvent the crude was chromatographed

on silica gel using dichloromethane as eluent to afford 0.5 g (77%) of a yellow powder. M.p.: 263–264 °C; <sup>1</sup>H NMR (300 MHz, CDCl<sub>3</sub>): δ = 9.87 (s, 1 H), 7.46–7.40 (m, 4 H), 7.25–7.16 (m, 7 H), 4.33–4.30 (m, 2 H), 4.21–4.19 ppm (m, 2 H); <sup>13</sup>C NMR (75 MHz, CDCl<sub>3</sub>): δ = 179.8, 148.4, 142.8, 138.8, 130.1, 127.6, 125.4, 125.2, 122.5, 116.5, 65.5, 64.6 ppm; HRMS (MALDI-TOF): elemental analysis calcd (%): 364.0882; found: 364.0875.

**(E)-2-((7-((2,2-Diphenylhydrazono)methyl)-2,3-dihydrothieno[3,4-b][1,4]dioxin-5-yl)methylene)malononitrile (4)**

A few drops of triethylamine was added to a mixture of **37** (0.46 g, 1.26 mmol) and malononitrile (0.125 g, 1.89 mmol) in 50 mL CHCl<sub>3</sub>. The reaction mixture was heated to 50 °C under argon atmosphere for 2 h. The solvent was evaporated and the residue was dissolved in dichloromethane, washed with water and brine and dried over MgSO<sub>4</sub>. After solvent removal, the crude was purified on silica gel using dichloromethane as eluent to give 0.44 g (85%) of a violet powder. M.p.: 229–230 °C; <sup>1</sup>H NMR (300 MHz, CDCl<sub>3</sub>): δ = 7.77 (s, 1 H), 7.48–7.42 (m, 4 H), 7.28–7.16 (m, 7 H), 4.35–4.33 (m, 2 H), 4.22–4.19 ppm (m, 2 H); <sup>13</sup>C NMR (75 MHz, CDCl<sub>3</sub>): δ = 148.8, 144.8, 142.5, 138.4, 130.2, 130.0, 125.9, 124.6, 122.6, 115.7, 114.5, 111.6, 71.1, 66.0, 64.6 ppm; HRMS (MALDI-TOF): elemental analysis calcd (%): 412.0994; found: 412.0987.

**(E)-1,1-Diphenyl-2-((2,2',3,3'-tetrahydro-[5,5'-bithieno[3,4-b][1,4]dioxin-7-yl)methylene)hydrazine (7e)**

To a solution of aldehyde **8e** (0.35 g, 1.13 mmol) in 100 mL dry THF heated to 66 °C was added dropwise a solution of *N,N'*-diphenylhydrazine hydrochloride (0.25 g, 1.13 mmol) and sodium acetate (0.18 g, 2.26 mmol) in 8 mL anhydrous methanol. The reaction mixture was refluxed during 24 h. After being cooled to room temperature, the mixture was quenched with water and dichloromethane. The aqueous layer was extracted twice with CH<sub>2</sub>Cl<sub>2</sub> and the combined organic extracts were dried over MgSO<sub>4</sub>. After solvent removal, the crude was purified by column chromatography on silica gel, using dichloromethane as eluent to afford 0.27 g (51%) of a yellow solid. M.p.: 252–253 °C; <sup>1</sup>H NMR (300 MHz, CDCl<sub>3</sub>): δ = 7.44–7.37 (m, 4 H), 7.32 (s, 1 H), 7.20–7.15 (m, 6 H), 6.29 (s, 1 H), 4.41–4.38 (m, 2 H), 4.29–4.25 (m, 4 H), 4.18–4.15 (m, 2 H); <sup>13</sup>C NMR (75 MHz, CDCl<sub>3</sub>): δ = 143.7, 141.5, 139.7, 137.6, 136.8, 129.9, 128.1, 124.5, 122.6, 113.6, 98.2, 65.2, 64.8 ppm; HRMS (MALDI-TOF): elemental analysis calcd (%): 476.0864; found: 476.0859.

**(E)-7'-((2,2-Diphenylhydrazono)methyl)-2,2',3,3'-tetrahydro-[5,5'-bithieno[3,4-b][1,4]dioxine]-7-carbaldehyde (6e)**

At 0 °C, anhydrous DMF (0.06 mL, 0.76 mmol) and phosphorus oxychloride (0.06 mL, 0.65 mmol) were added to a solution of hydrazone derivative **7e** (0.26 g, 0.54 mmol) in 30 mL 1,2-dichloroethane. The mixture was stirred, overnight, at room temperature under argon atmosphere. A saturated aqueous solution of sodium acetate and dichloromethane were added and the solution was additionally stirred for 2 h. The aqueous layer was extracted twice with CH<sub>2</sub>Cl<sub>2</sub>; the combined organic extracts were washed with water and brine, and then dried over MgSO<sub>4</sub>. Solvent removal and column chromatography on silica gel (eluent: dichloromethane) gave 0.18 g (65%) of an orange solid. M.p.: 276–277 °C; <sup>1</sup>H NMR (300 MHz, CDCl<sub>3</sub>): δ = 9.90 (s, 1 H), 7.45–7.39 (m, 4 H), 7.28 (s, 1 H), 7.22–7.17 (m, 6 H), 4.48–4.42 (m, 4 H), 4.34–4.31 (m, 2 H), 4.20–4.18 ppm (m, 2 H); <sup>13</sup>C NMR (75 MHz, CDCl<sub>3</sub>): δ = 179.6, 148.1, 143.4, 140.0, 139.5, 136.6, 130.0, 127.2, 124.8, 122.6, 122.1, 117.9, 115.4,

108.7, 65.5, 65.4, 65.0, 64.7 ppm; HRMS (MALDI-TOF): elemental analysis calcd (%): 504.0814; found: 504.0812.

**(E)-2-((7'-((2,2-Diphenylhydrazono)methyl)-2,2',3,3'-tetrahydro-[5,5'-bithieno[3,4-b][1,4]dioxin]-7-yl)methylene)malononitrile (5)**

Malonodinitrile (21 mg, 0.64 mmol) and a few drops of triethylamine were added to a solution of aldehyde **6e** (160 mg, 0.32 mmol) in 30 mL chloroform and the mixture was stirred, overnight, at ambient temperature. After solvent removal the residue was dissolved in dichloromethane, washed with water, brine and dried over MgSO<sub>4</sub>. The crude was chromatographed on silica gel using dichloromethane as eluent yielding 170 mg (96%) of a deep violet powder. M.p.: 308–309 °C; <sup>1</sup>H NMR (300 MHz, CDCl<sub>3</sub>): δ = 7.76 (s, 1 H), 7.47–7.41 (m, 4 H), 7.24–7.17 (m, 7 H), 4.49–4.47 (m, 2 H), 4.43–4.38 (m, 4 H), 4.22–4.19 ppm (m, 2 H); <sup>13</sup>C NMR (75 MHz, CDCl<sub>3</sub>): δ = 148.5, 144.2, 143.1, 141.2, 139.6, 136.2, 130.1, 126.5, 125.2, 122.5, 120.3, 116.2, 115.3, 111.4, 110.7, 108.4, 68.3, 65.9, 65.7, 64.9, 64.7 ppm; HRMS (FAB): elemental analysis calcd (%): 552.0926; found: 552.0917.

**Device fabrication and testing**

Indium–tin oxide coated glass slides of 24 mm × 25 mm × 1.1 mm dimensions with a surface resistance of 10 Ω per square were purchased from Kintec company. Part of the ITO layer was etched away with 37% HCl. The ITO electrodes were then cleaned in an ultrasonic bath with, successively, Deconex (VWR international GmbH), distilled water (15.3 MΩ cm<sup>-1</sup>), acetone, ethanol and distilled water for 10 min each wash, and dried in an oven at 100 °C. The dried electrodes were then modified by a spun-cast layer of PEDOT:PSS (Clevios P VP. Al 4083 (HC-Starck) filtered through a 0.45 μm membrane just prior use). Spin-casting was achieved at 5000 rpm (*r* = 10 s, *t* = 60 s), and the electrode was then dried at 130 °C for 15 min. Films of donor materials (ca. 20 nm) were spun-cast in atmospheric conditions from chloroform solutions containing 4 mg donor per mL. After film deposition the devices were introduced in an argon glovebox (200B, MBraun) equipped with a vacuum chamber and a 30 nm film of Fullerene C<sub>60</sub> (99+%; MER Corporation) and a 100 nm thick aluminium electrode were thermally evaporated on top of the donor film under a pressure of 2 × 10<sup>-6</sup> mbar through a mask defining two cells of 6.0 mm diameter (0.28 cm<sup>2</sup>) on each ITO electrode.

The *J* versus *V* curves of the devices were recorded in the dark and under illumination using a Keithley 236 source-measure unit and a homemade acquisition program. The light source was an AM1.5 Solar Constant 575 PV simulator (Steuernagel Lichttechnik, equipped with a metal halogen lamp). For each measurement the incident light intensity (ca. 90 mW cm<sup>-2</sup>) was measured by a broadband power meter (13PEM001, Melles Griot). The devices were illuminated through the ITO electrode side. The efficiency values reported here are not corrected for the possible spectral mismatch of the solar simulator. External quantum efficiency (EQE) was measured using a halogen lamp (Osram) with an Action Spectra Pro 150 monochromator, a lock-in amplifier (PerkinElmer 7225) and a S2281 photodiode (Hamamatsu).

**Acknowledgements**

The authors thanks the French “Ministère des affaires étrangères” for the Eiffel grant for A.D.

**Keywords:** basic condensation · clean chemistry · donor-acceptor systems · organic solar cells · photochemistry

- [1] Y.-J. Cheng, S. H. Yang, C.-S. Hsu, *Chem. Rev.* **2009**, *109*, 5868.  
 [2] Y. Liang, L. Yu, *Acc. Chem. Res.* **2010**, *43*, 1227.  
 [3] Y. Li, *Acc. Chem. Res.* **2012**, *45*, 723.  
 [4] a) C. W. Tang, *Appl. Phys. Lett.* **1986**, *48*, 183; b) D. Wöhrle, D. Meissner, *Adv. Mater.* **1991**, *3*, 129; c) P. Peumans, A. Yakimov, S. R. Forrest, *J. Appl. Phys.* **2003**, *93*, 3693.  
 [5] a) G. Yu, J. Gao, J. C. Hummelen, F. Wudl, A. J. Heeger, *Science* **1995**, *270*, 1789; b) J. J. M. Halls, C. A. Walsh, N. C. Greenham, E. A. Marseglia, R. H. Friend, S. C. Moratti, A. B. Holmes, *Nature* **1995**, *376*, 498; c) S. Günes, H. Neugebauer, N. S. Sariciftci, *Chem. Rev.* **2007**, *107*, 1324; d) C. J. Brabec, S. Gowrisanker, J. J. M. Halls, D. Laird, S. Jia, S. P. Williams, *Adv. Mater.* **2010**, *22*, 3839.  
 [6] a) J. Roncali, *Acc. Chem. Res.* **2009**, *42*, 1719; b) F. Würthner, K. Meerholz, *Chem. Eur. J.* **2010**, *16*, 9366; c) Y. Li, Q. Guo, Z. Li, J. Pei, W. Tian, *Energy Environ. Sci.* **2010**, *3*, 1427; d) B. Walker, C. Kim, T.-Q. Nguyen, *Chem. Mater.* **2011**, *23*, 470; e) Y. Lin, Y. Li, X. Zhan, *Chem. Soc. Rev.* **2012**, *41*, 4245; f) J. Roncali, P. Leriche, P. Blanchard, *Adv. Mater.* **2014**, *26*, 3821.  
 [7] a) Y. Y. Liang, Z. Xu, J. B. Xia, S. T. Tsai, Y. Wu, G. Li, C. Ray, L. P. Yu, *Adv. Mater.* **2010**, *22*, E135; b) Z. He, C. Zhong, S. Su, M. Xu, H. Wu, Y. Cao, *Nat. Photonics* **2012**, *6*, 591; c) C. Cabanetos, A. El Labban, J. A. Barteld, J. D. Douglas, W. M. Mateker, J. M. J. Fréchet, M. D. McGehee, P. M. Beaujuge, *J. Am. Chem. Soc.* **2013**, *135*, 4656.  
 [8] a) V. Steinmann, N. M. Kronenberg, M. R. Lenze, S. M. Graf, D. Hertel, K. Meerholz, H. Bürckstümmer, E. V. Tulyakova, F. Würthner, *Adv. Energy Mater.* **2011**, *1*, 888; b) R. Fitzner, E. Mena-Osteritz, A. Mishra, G. Schulz, E. Reinold, M. Weil, C. Körner, H. Ziehlke, C. Elschner, K. Leo, M. Riede, M. Pfeiffer, C. Ulrich, P. Bäuerle, *J. Am. Chem. Soc.* **2012**, *134*, 11064; c) L.-Y. Lin, Y.-H. Chen, Z.-Y. Huang, H.-W. Lin, S.-H. Chou, F. Lin, C.-W. Chen, Y.-H. Liu, K.-T. Wong, *J. Am. Chem. Soc.* **2011**, *133*, 15822; d) Y.-H. Chen, L.-Y. Lin, C.-W. Lu, F. Lin, Z.-Y. Huang, H.-W. Lin, P.-H. Wang, Y.-H. Liu, K.-T. Wong, J. Wen, D. J. Miller, S. B. Darling, *J. Am. Chem. Soc.* **2012**, *134*, 13616.  
 [9] a) Y. Sun, G. C. Welch, W. L. Leong, C. J. Takacs, G. C. Bazan, A. J. Heeger, *Nat. Mater.* **2011**, *11*, 44; b) J. Zhou, Y. Zuo, X. Wan, G. Long, Q. Zhang, W. Ni, Y. Liu, Z. Li, G. He, C. Li, B. Kan, M. Li, Y. Chen, *J. Am. Chem. Soc.* **2013**, *135*, 8484; c) S. Shen, P. Jiang, C. He, J. Zhang, P. Shen, Y. Zhang, Y. Yi, Z. Zhang, Z. Li, Y. Li, *Chem. Mater.* **2013**, *25*, 2274.  
 [10] a) D. J. Burke, D. J. Lipomi, *Energy Environ. Sci.* **2013**, *6*, 2053; b) T. P. Ose-dach, T. L. Andrew, V. Bulovic, *Energy Environ. Sci.* **2013**, *6*, 711; c) G. Marziano, C. V. Ciasca, F. Babudri, G. Bianchi, A. Pellegrino, R. Po, G. M. Fari-nola, *Eur. J. Org. Chem.* **2014**, 6583.  
 [11] H. E. Katz, Z. Bao, S. L. Gilat, *Acc. Chem. Res.* **2001**, *34*, 359.  
 [12] a) A. Leliège, D. Demeter, V. Jeux, T. Rousseau, P. Leriche, P. Blanchard, J. Roncali, *Chem. Eur. J.* **2013**, *19*, 9948; b) D. Demeter, V. Jeux, P. Leriche, P. Blanchard, Y. Olivier, J. Cornil, R. Po, J. Roncali, *Adv. Funct. Mater.* **2013**, *23*, 4854; c) V. Jeux, D. Demeter, P. Leriche, J. Roncali, *RSC Adv.* **2013**, *3*, 5811; d) D. Demeter, S. Mohamed, A. Diac, I. Grosu, J. Roncali, *ChemSusChem* **2014**, *7*, 1046.  
 [13] J. Roncali, L. Rasmussen, C. Thobie-Gautier, P. Frère, M. Sallé, H. Brisset, A. Gorgues, M. Jubault, J. Becher, J. Orduna, *Adv. Mater.* **1994**, *6*, 841.  
 [14] a) M. Turbiez, P. Frère, M. Allain, C. Vidlot, J. Ackerman, J. Roncali, *Chem. Eur. J.* **2005**, *11*, 3742; b) J. Roncali, P. Frère, P. Blanchard, R. de Bettignies, M. Turbiez, S. Roquet, P. Leriche, Y. Nicolas, *Thin Solid Films* **2006**, *511–512*, 567.  
 [15] D. Demeter, T. Rousseau, J. Roncali, *RSC Adv.* **2013**, *3*, 704.  
 [16] D. Baran, A. Balan, S. Celebi, B. Meana Esteban, H. Neugebauer, N. S. Sar-iciftci, L. Toppare, *Chem. Mater.* **2010**, *22*, 2978.  
 [17] R. N. Adams, *Acc. Chem. Res.* **1969**, *2*, 175.  
 [18] J. W. Choi, C. H. Kim, J. Pison, A. Oyedele, H. Derbal-Habak, D. Tondelier, A. Leliège, E. Kirchner, P. Blanchard, J. Roncali, B. Geffroy, *RSC Adv.* **2014**, *4*, 5236.  
 [19] P. Leriche, J.-M. Raimundo, M. Turbiez, V. Monroche, M. Allain, F.-X. Sauv-age, J. Roncali, P. Frère, P. J. Skabara, *J. Mater. Chem.* **2003**, *13*, 1324.  
 [20] G. A. Sotzing, C. A. Thomas, J. R. Reynolds, *Macromolecules* **1998**, *31*, 3750.  
 [21] J.-M. Raimundo, P. Blanchard, P. Frère, N. Mercier, I. Ledoux-Rak, R. Hierle, J. Roncali, *Tetrahedron Lett.* **2001**, *42*, 1507.  
 [22] CCDC 1026342 (1), 1026343 (2), 1026344 (3), contain the supplementary crystallographic data for this paper. These data can be obtained free of charge from The Cambridge Crystallographic Data Centre via [www.ccdc.cam.ac.uk/data\\_request/cif](http://www.ccdc.cam.ac.uk/data_request/cif).

Received: September 26, 2014  
 Published online on ■■■■■, 0000

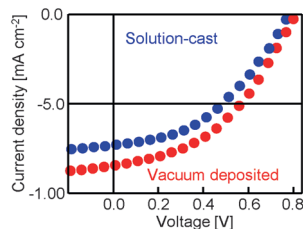
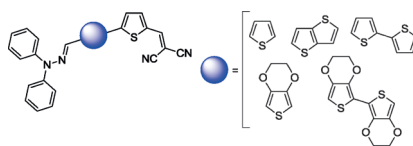
## FULL PAPER

### Photochemistry

A. Diac, D. Demeter, M. Allain, I. Grosu,  
J. Roncali\*



Simple and Versatile Molecular Donors  
for Organic Photovoltaics Prepared by  
Metal-Free Synthesis



**Finding the right partner:** Small push-pull molecules were synthesized in good yields by a three-step metal-free procedure. Thin films produced by both solution process and vacuum deposition led to interesting photovoltaic performances in simple bilayer heterojunction solar cells with C<sub>60</sub> as acceptor material.